

IFUSP/P 330  
B.I.F. - USP

UNIVERSIDADE DE SÃO PAULO

INSTITUTO DE FÍSICA  
CAIXA POSTAL 20516  
01000 - SÃO PAULO - SP  
BRASIL

# publicações

IFUSP/P-330

INTERMICELLAR INTERACTIONS IN TYPE I LYOTROPIC  
"NEMATIC" LIQUID CRYSTALS

by

A.M. Figueiredo Neto and L.Q. Amaral

Instituto de Física, Universidade de São Paulo,  
C.P. 20516, São Paulo, SP, Brazil

**B.I.F. - USP**

Abril/1982

INTERMICELLAR INTERACTIONS IN TYPE I LYOTROPIC "NEMATIC" LIQUID CRYSTALS

by A.M.FIGUEIREDO NETO AND L.Q.AMARAL

INSTITUTO DE FÍSICA, UNIVERSIDADE DE SÃO PAULO  
CP: 20516, SÃO PAULO, CEP 05508, BRAZIL

INTERMICELLAR INTERACTIONS IN "NEMATICS"

A.M.FIGUEIREDO NETO

INSTITUTO DE FÍSICA, UNIVERSIDADE DE SÃO PAULO  
CP: 20516, SÃO PAULO, CEP 05508, BRAZIL

NUMBER OF MANUSCRIPT PAGES: 19

NUMBER OF TABLES: 1

NUMBER OF FIGURES: 8

ABSTRACT

The application of classical DLVO theory to a type I lyomesophase indicates that the cylindrical amphiphilic micelles tend to flocculate; the screening process is so efficient that the van der Waals attractive force is higher than the coulombian repulsive one (this later caused by the ionization of the micellar surface polar groups). The flocculation process forms a hexagonal network with lattice parameter (determined by X-ray diffraction technique) of  $49.9\text{\AA}$ . This result can be explained assuming that the micelles have a bound solvation shell around them about  $8\text{\AA}$  thick. The balance between van der Waals attraction and excluded volume interaction is responsible for the aggregation process. The calculated energy of two interacting micelles  $50\text{\AA}$  apart is about  $KT$ , indicating that at the bulk of the lyomesophase only small aggregates can exist. However, external agents like electric and magnetic fields or wall containers, which restrict degrees of freedom of the micelles, favours flocculation. The container wall effect is described as a micellar anchoring process.

## I - INTRODUCTION

Lyotropic liquid crystalline phases that spontaneously orient in presence of magnetic fields ( $\vec{H}$ ) have been classified by NMR experiments as types I and II [1,2], depending on whether the phase director orients respectively parallel or perpendicular to  $\vec{H}$ . Observations of its optical textures in a polarized microscope, which resemble nematic ones, were used [3-5] to characterize these mesophases as nematics.

Amaral and co-workers [6-8] studied a type II lyomesophase by small angle X-ray scattering, proposing a model of finite planar micelles, in the form of platelets, not homogeneously distributed in water, forming lamellar aggregates.

Type I lyomesophases of potassium laurate/KCl/water (called LK) and of cesium decylsulfate/CsNO<sub>3</sub>/water (called CDS) were studied [9] by X-ray diffraction and polarized optical microscopy techniques, in several experimental conditions: samples in different sample holders and submitted to electric and magnetic fields. The results with magnetically oriented samples confirm [9] the model of long cylindrical micelles previously proposed [2,3] (length bigger than 500Å) and also indicate the existence of aggregates of micelles separated by the excess water. A typical photographing diffraction result with sample LK in glass capillaries of 0.7 mm diameter presents two bands [9] at the s (absolute value of the scattering vector) position of  $(40\text{Å})^{-1}$ , named outer band (OB), and  $(100\text{Å})^{-1}$ , named inner band (IB), while the same samples in 2 mm thick capillaries present only IB. The analysis of these results was made assuming non homogeneous distribution of micelles in water. In a previous paper [10], the model of aggregates of micelles was quantitatively developed: the micelles have cylindrical

shape with radius of 17Å and are packed in an hexagonal lattice of parameter  $(49.9 \pm 0.5)\text{Å}$ ; OB was associated to the 100 diffraction peak of the array for aggregates of about one hundred micelles and IB was associated to the mean distance among smaller aggregates (about three or four micelles each). In this picture, the "nematic" type I phase could be thought as composed by microdomains of the lyotropic conventional middle soap phase ( $H_a$ ).

Recent X-ray diffraction results with sample LK in different temperatures [11,12] show the coexistence of two phases (type I and  $H_a$ ) for temperatures between 50 and 60°C.

The effect of the container walls [9] also play a significant role in the formation of the large aggregates. The higher intensity of OB compared to IB for thinner capillaries corroborate this fact.

Besides temperature and container wall effect, electric [9] and magnetic [11] applied fields also favour the formation of large aggregates.

Up to now, there was nothing about the process of formation of such aggregates, i.e., the kind of intermicellar interactions responsible for the stability of the system has not been discussed. Specifically for the type I LK phase, there are cylindrical micelles of amphiphilic (with the ionizable polar group at the surface surrounding the paraffinic region) immersed in an ionic bathing medium of water and salt. The interplay between van der Waals attractive and coulombian repulsive forces are usually employed to describe similar systems like colloids and biological membranes [13,14]. The possible applicability of this approach to the lyotropes was mentioned before [14,15], however it was not made yet.

In this paper we discuss the intermicellar interactions based on the balance of van der Waals attractive and coulombian repulsive forces between micelles, adding considerations about the solvation water [15] (water bounded to the micelles) for type I "nematic" liquid crystals and present some complementary experimental results with sample LK to corroborate the proposed picture for the system stability.

## II - INTERACTION FORCES BETWEEN CYLINDRICAL POLYELECTROLYTES IN AN IONIC SOLUTION

### II.1 - GENERAL CONSIDERATIONS

The theory of Debye-Hückel [16] has been successfully used to describe the thermodynamics of solutions of strong electrolytes. The theory for the computation of the repulsive force begins with the Poisson equation, where the volumetric charge density of the solution is introduced in a convenient form [16] and, in the mean field approximation for the computation of the force acting on an ion due to the others, the non linear Poisson-Boltzmann (PB) equation is obtained. Another approximation is usually done in PB equation that consists in its linearization with obtainment of the well known linearized Poisson-Boltzmann equation (LPB) [16, 17]. These approximations are totally justified at the low ion concentration limit [14,16-18], i.e., diluted solution. This concentration is usually expressed in terms of the ionic strength (I) defined as  $I = \frac{1}{2} \sum_i \rho_i z_i^2$  where  $\rho_i$  is the ion concentration,  $z_i$  its charge in terms of the electron charge

and the summation performed over all the ionic species. The ionic strength upper limit for the applicability of the LPB equation is not fixed, depending on the particular system; however,  $I \sim 0.1 \text{ mol dm}^{-3}$  is already considered [14] a high value. A complete review about this point was made by Olivares and McQuarrie [17].

The Debye-Hückel theory for the computation of the repulsive interaction is largely used [14] in connection to the classical theory of Derjaguin, Landau, Verwey and Overbeek (DLVO) to describe the stability of colloidal and biological systems. Specially for systems whose particles have cylindrical shape [14,18-21] the mathematical difficulties lead to the utilization of the LPB equation.

Sparnaay [21] discussed the interaction between two cylindrical particles with an homogeneous surface charge density immersed in an ionic bathing medium. The attractive component, following DLVO theory, was calculated [21] by summation of van der Waals pair interactions and the attractive potential is left in terms of an adjustable constant (Hamaker constant). The stability of the system was determined by the two forces balance [21] and for high ionic strength the screening of the charged surfaces is so efficient that the system flocculates.

Brenner and McQuarrie [14] discussed two systems of cylindrical shaped particles (gels of tobacco mosaic virus and the A band lattice of myosin in vertebrate striated muscle) assuming non homogeneous charge distribution; the electrostatic potential at the particle surface depends on the charge distribution on it and the charge is itself a function of the potential. The surface charge density was determined [14] applying the boundary condition in a self-consistent

way. This treatment has many advantages compared to the Sparnaay one, however a limitation of it is the necessary knowledge of the dissociation constant of the ionizable groups at the particle surface [14]. In the calculation of the attractive interaction the same pairwise summation method was employed [14], however a value from the literature for the Hamaker constant was introduced, with the advantage that this value was obtained using Lifshitz theory.

In the study of the "nematic" lyomesophases we adopt an intermediary approach. At the surface of the micelles (sample LK) there are carboxilate groups that in presence of water are in principle totally ionized; the counter ions can be totally or partially bound at the micellar interface but there is not a defined dissociation constant in this particular situation. This fact prevents the use of the Brenner-McQuarrie formalism in its original form for the computation of the repulsion and we assume an homogeneous charge distribution. However for the computation of the attractive force, we adopt Brenner-McQuarrie scheme.

Besides this two forces balance the stability of colloids which have water affinity needs considerations about solvation water [13] (water molecules bounded to the colloid or to the ionic double-layers surrounding it). In lyomesophases this point is of fundamental importance since the micelles have polar groups in its surface and are surrounded by a counter ions screening cloud.

It was recently demonstrated [22] that the bathing medium structure (basically the solvent) is of fundamental importance, modifying the classical approach

for the computation of the attractive force. This fact is particularly important when interparticle distances are comparable to the dimensions of the solvent molecule [22]. Theoretical treatments to solvation forces have been recently published [23], modifying the classical DLVO approach. In this paper these new theories won't be used.

## II.2 - Coulombian repulsive interaction

The system is composed by two long parallel cylinders with radius  $R$  and length  $L$  ( $L \gg R$ ), immersed in a bathing medium of known ionic strength. The distance between their axis is  $D$ . They are rigid and composed by a material of dielectric constant  $\epsilon_i$ , have uniform density and the surface charge is homogeneously distributed. The bathing medium has a dielectric constant  $\epsilon \gg \epsilon_i$  and the temperature is constant ( $T$ ).

From the LPB equation for a single cylinder, and defining  $\frac{1}{\kappa}$  as the Debye-Screening length:

$$\kappa^2 = \frac{8\pi e^2}{\epsilon KT} I \quad 1$$

where  $e$  is the electron charge and  $K$  the Boltzmann constant, it is possible [14] to write an expression for the electrostatic potential at the position  $\vec{r}$  from the center of the cylinder  $\psi(\vec{r})$  in terms of a single unknown constant. For the whole system, by superposition we have in the zero order approximation [14]:

$$\psi^{(0)}(\vec{r}) = A_0^{(0)} \left\{ K_0(\kappa r) + \sum_{n=-\infty}^{\infty} K_n(\kappa D) I_n(\kappa r) \cos(n\theta) \right\}$$

where  $\theta$  is the polar angle of a coordinate system placed at one of the cylinders,  $I_n$  and  $K_n$  are the modified Bessel functions of 1<sup>st</sup> and 2<sup>nd</sup> kind respectively and order  $n$ .

Applying the boundary condition, the discontinuity of the normal component of the electric field at the cylinders surface, the constant  $A_0^{(o)}$  is obtained in terms of the charge density  $\sigma$ . This density can be expressed in terms of the surface per ionizable group ( $S$ ) and its degree of dissociation ( $\alpha$ ). So,  $A_0^{(o)}$  can be written:

$$A_0^{(o)} = \frac{4\pi e \alpha}{\epsilon S \kappa} \{K_1(\kappa R) - K_0(\kappa D) I_1(\kappa R)\}^{-1} \quad 3$$

In the expression for the Gibbs free energy of the system, only the electrostatic [24] term (in this approximation) depends on  $D$ . With this consideration and the expressions 2 and 3 a straightforward calculation gives for the repulsive force per unit length of the cylinder  $F_r(D)$

$$F_r(D) = 2\pi R \frac{e\alpha}{S} \frac{\partial}{\partial D} \psi^{(o)} \quad , 4$$

$$F_r(D) = .2\pi R \frac{e\alpha}{S} \{a.b+c\} \quad , 5$$

where  $a = -\frac{4\pi e \alpha}{\epsilon S} I_1(\kappa R) K_1(\kappa D) \{K_1(\kappa R) - K_0(\kappa D) I_1(\kappa R)\}^{-2}$

$$b = K_0(\kappa R) + K_0(\kappa D) I_0(\kappa R)$$

$$c = -A_0^{(o)} I_0(\kappa R) \kappa K_1(\kappa D)$$

This force can be well fitted [25] by a function

$$F_r(D) = \frac{\gamma e^{-\kappa D}}{\sqrt{\kappa D}} \quad , 6$$

where  $\gamma$  is a force parameter. From this expression it is possible to write down the electrostatic potential energy

of the system  $V_r(D)$  as:

$$V_r(D) = \frac{\sqrt{\pi} \gamma}{\kappa} \operatorname{erfc}(\sqrt{\kappa D}) \quad , 7$$

where  $\operatorname{erfc}$  is the complementary error function.

### II.3 - VAN DER WAALS ATTRACTIVE INTERACTION

For the computation of the force and potential energy we follow the scheme proposed by Brenner and McQuarrie [14] with a pairwise summation of interactions. The basic energy interaction between two atoms separated by the distance  $r$  is

$$v(r) = -C_6 r^{-6} \quad , 8$$

where  $C_6$  is the characteristic interaction constant. Summing over all the atoms of the two cylinders [14], we obtain the total interaction energy per unit length of the cylinders  $V_a(D)$  in terms of the Hamaker constant ( $A$ ):

$$V_a(D) = -\frac{2A}{3D} \sum_{m=1}^{\infty} \sum_{n=1}^{\infty} \frac{\Gamma^2(m+n+1/2)}{m! n! (m-1)! (n-1)!} \left(\frac{R}{D}\right)^{2(m+n)} \quad , 9$$

where  $\Gamma$  is the gamma function; and for the attractive force per unit length:

$$F_a(D) = -\frac{2A}{3D^2} \sum_{m=1}^{\infty} \sum_{n=1}^{\infty} \frac{[\Gamma^2(m+n+1/2)] (2m+2n+1)}{m! n! (m-1)! (n-1)!} \left(\frac{R}{D}\right)^{2(m+n)} \quad , 10$$

### III - EXPERIMENTAL

Mesophase LK was prepared [1,2] by the NMR

Laboratory of the Instituto de Química da USP with the

following composition: K laurate ( $34.49 \pm 0.06$ ) wt%/KCl ( $2.94 \pm 0.01$ ) wt%/H<sub>2</sub>O ( $62.6 \pm 0.1$ ) wt%.

Samples were sealed in several containers

- C1 - quartz capillary with 0.3 mm diameter;
- C2 - quartz capillary with 0.5 mm diameter;
- C3 - quartz capillary with 0.7 mm diameter;
- C4 - lindemann glass capillary with 0.7 mm diameter;
- C5 - pirex glass capillary with 2 mm diameter;
- C6 - cylindrical container with very thin parallel walls of niquel (or mylar) with 6 mm diameter and sample thickness of 0.7 and 2 mm.

Samples in capillary C5 were magnetically oriented in permanent magnets of 14 kG and 2 kG and afterwards analysed by small angle X-ray scattering and optical microscopy. Residual magnetic orientation was observed, i.e., the field was not present during the X-ray exposure.

X-ray diffraction patterns were obtained by photographing technique using a small angle Rigaku-Denki diffractometer with Cu K<sub>α</sub> radiation (Ni filtered) in a transmission geometry with point focus.

The capillary was always placed in the vertical direction, with their axis perpendicular to the X-ray beam, which at the sample position had a diameter of 0.3 mm. So, only capillary C1 is embraced by the beam, while the others received the beam in their central part. Exposure times varied between 24 to 48 hours, depending on sample thickness. All results were obtained at room temperature ( $\sim 22^\circ\text{C}$ ).

Some of the results were obtained with capillaries of chemically treated surfaces. Three types of treatments were performed:

T1: with sulphocromic solution. The solution is introduced in the capillaries for a period of 24 hours, followed by a continuous flux of destilated water (some hours). During the process there is a deposition of ions Cr<sup>3+</sup>, CrO<sub>4</sub><sup>2-</sup>, K<sup>+</sup> at the surface, that are removed by the water flux. The treatment consists in removing all the organic material present at the surface (a cleaning treatment).

T2: with NaOH. The process consist in filling the capillary with a solution of NaOH in 10 vol% for a period of some days. Afterwards, a flux of destilated water with 0.001 mol dm<sup>-3</sup> of NaOH passes throw the capillary for hours. The OH groups at the glass surface are substituted by ONa groups.

T3: with (H<sub>3</sub>C)<sub>2</sub> SiCl<sub>2</sub>. The process consist in filling the capillary with the substance and shake it for some minutes. The residual substance volatilizes very quickly. The chemical reaction is very efficient and promote the location of apolar CH<sub>3</sub> groups at the glass surface, which becomes hydrophobic.

#### IV - EXPERIMENTAL RESULTS

Comparing the diffraction patterns of sample LK in capillary C5 with and without residual magnetic orientation, it was observed a dislocation of IB position to smaller values of  $2\theta$  for magnetically oriented samples indicating the formation of aggregates with aggregation number (N) bigger than 4. As discussed elsewhere [9], the field aligns

the micelles with their axis parallel to it, imposing restrictions to the micellar degrees of freedom.

Diffraction patterns obtained with sample LK in very thin capillaries C1 and C2 (Fig.1 and 2 respectively), where the surface effect is intensified, are composed by Bragg points at OB region and weak lines (not visible at the reproduction) with characteristic distance  $\frac{1}{\sqrt{3}}$  of the Bragg point one. The hexagonal lattice parameter obtained is  $(46.4 \pm 0.5) \text{ \AA}$ . A visual mesure (using a Rigaku-Denki nonio) of the Bragg points width, of the order of the experimental resolution (about  $0.20^\circ$ ) indicates [10,11] that the structures responsible for this diffraction pattern are very large compared to the aggregates of  $N \sim 100$  associated to OB; they have about 400 aggregated micelles or more. So, the surface effects in thin capillaries favour the formation on bigger aggregates of micelles. The preferred equatorial orientation of the Bragg points at OB region indicates that the micellar axes are oriented preferentially parallel to the capillary axis.

The equatorial orientation is due to the geometry of the container. Samples in capillary C3 present IB and OB with equatorial orientation while in parallel walls container C6 (with the same sample thickness) the bands do not present this orientation (Fig.3). The same phenomenon was observed in capillary C5 and container C6 with the same sample thickness. The material of the walls (niquel or mylar) does not influence the diffraction pattern.

To clarify the container wall effect in terms of the formation of the aggregates some surface chemical treatments were performed. Treatment T1 in capillaries C3,C4

and C5 do not modify the usual [9] diffraction patterns, indicating that no organic deposit (removed with T1) could be responsible for the surface effect. Treatment T2 in capillary C5 also does not modify the usual [9] diffraction pattern, indicating that the substitution of the hydrogen by sodium at the surface does not modify wall effect. Treatment T3 in capillaries C3, C4 and C5 (Fig.4 and 5), however, presents different patterns. With 0.7 mm thick capillaries there are Bragg points at OB region and weak lines (not visible at the reproduction) with characteristic distance  $\frac{1}{\sqrt{3}}$  of the Bragg point one (Fig.4). The hexagonal lattice parameter obtained from these diffractions is  $(48.8 \pm 0.6) \text{ \AA}$ ; IB is transformed in radial streaks. As discussed elsewhere [9,11,12], part of the streaks intensity may be due to white radiation, always present in Ni filtered radiation, however this contribution is not the principal. With 2 mm thick capillary (Fig.5), besides IB there are radial streaks present and in some directions very weak points at OB region (they are not visible in the reproduction). The streaks indicates the existence of some preferred orientations for phase directors of the small aggregates ( $N \sim 4$ ) and the appearance of Bragg points at OB region indicates the formation of large aggregates induced by surface treatment. As discussed before, treatment T3 promotes the location of apolar  $\text{CH}_3$  groups at the capillary surface. The hydrophobicity of the treated surface favours the segregation of free water (not directly bounded to the micelles) from its proximity and large aggregates of micelles can be formed. The lattice parameter obtained for these superaggregates ( $N \sim 400$ ), considering the experimental



errors, is equal to that obtained for the aggregates of about 100 micelles. Probably the treated surface excludes from its proximity the free water and favour the growing of the N-100 aggregate "seeds", without a fundamental modification of the lattice parameter.

## V - ANALYSIS OF MICELLAR STABILITY

### (A) - REPULSIVE COULOMBIAN INTERACTION

LK micelles are constituted by a cylindrical hydrophilic shell and a core of hydrocarbon. In the hydrophilic region there are polar groups  $\text{COO}^- \text{K}^+$ . The micelles are immersed in a bathing medium composed by the water; counter ions  $\text{K}^+$  of the surface polar groups ionization and ions  $\text{K}^+$  and  $\text{Cl}^-$  from the salt. The molarities of the components of the mesophase were calculated in an usual procedure (in moles of the component per  $\text{dm}^3$  of the solvent), with the composition given in section III: for the water  $(55.49 \pm 0.09) \text{ mol dm}^{-3}$ ; for the K laurate  $(2.31 \pm 0.01) \text{ mol dm}^{-3}$  and for the salt  $(0.63 \pm 0.01) \text{ mol dm}^{-3}$ .

In a first approach, assuming that all the surface polar groups and the salt are ionized, the ionic strength of the bathing medium (section II.1) is  $(1.79 \pm 0.06) \text{ mol dm}^{-3}$ . The Debye screening length associated to this value assuming a temperature of  $25^\circ\text{C}$  and the value 78.5 for the dielectric constant of the medium [25] is  $(2.27 \pm 0.04) \text{ \AA}$ . This parameter informs how efficient is the electrostatic screening of the micelles [16]; so, the counter ions are brought near to the surface in such a manner that

at about  $3\text{ \AA}$  apart from it the micelles are totally involved by the ions  $\text{K}^+$ . This length is of the order of the distance between the residual group  $\text{COO}^-$  and the  $\text{K}^+$  in the molecule of K laurate [26]; so, the system may be thought as weakly charged. The hypothesis of counter ions totally bound to the micelles is usually assumed in the hexagonal phase [15]. With this very small Debye length, we can consider an effective ionization coefficient ( $\alpha$ ) very small, corresponding to a micellar system highly screened. At the limit of  $\alpha \rightarrow 0$  the ionic strength is  $0.63 \text{ mol dm}^{-3}$ , due to the salt. The value of  $1.79 \text{ mol dm}^{-3}$  for the ionic strength prevents the utilization of the classical Debye-Hückel theory, however, at the inferior limit  $0.63 \text{ mol dm}^{-3}$ , the use of the LPB equation is not so drastic. The mathematical difficulties of an alternative [17] treatment (with the necessary approximations) justifies this easier approach.

Expression 5 for the repulsive force per unit length as a function of the interaxial distance D was computed for

$$\alpha = 0.02; 0.05; 0.1; 0.15; 0.20; 1$$

and in Fig. 6  $\ln F_r$  is plotted as a function of D. The bigger the value of  $\alpha$  the worst is the result in terms of the utilization of the LPB equation.

For the computation of the potential energy we assume expression 6 for the force to obtain the force parameter  $\gamma$  and afterwards use expression 7. In Table I we present the relation between the forces calculated by expressions 5 and 6 to give an idea of the approximation.

TABLE I

$F_r/F_{ra}$ \ D(Å)	40	50	60	70	80	90	100
$\alpha = 0.2$	0.76	0.81	0.89	0.98	1.08	1.19	1.32
$\alpha = 0.15$	1.04	1.00	1.00	1.00	0.99	0.99	0.98
$\alpha = 0.10$	1.05	1.01	1.00	1.00	1.00	0.99	0.99
$\alpha = 0.05$	0.77	0.81	0.89	0.99	1.08	1.19	1.32
$\alpha = 0.02$	0.77	0.81	0.89	0.99	1.08	1.19	1.31

TABLE I: Values of the relation  $F_r/F_{ra}$ , where  $F_r$  is the exact repulsive force obtained from LPB equation and  $F_{ra}$  is the approximation (c.f. expression 6), as a function of the interaxial distance (D), for different values of the dissociation constant ( $\alpha$ ).

#### (B) ATTRACTIVE VAN DER WAALS INTERACTION

The attractive interaction acts between the two cylindrical hydrocarbon cores separated by water. The utilization of expressions 9 and 10 depends on finding a reasonable value for the Hamaker constant. Gingell and Parsegian [27,28] studied a system composed by two semi-infinite layers of water separated by hydrocarbon; using spectroscopic data and Lifshitz theory, they obtained a range of variation of the constant A for the system hydrocarbon-water, from  $3.4$  to  $6.8 \times 10^{-14}$  erg. Despite the geometric differences of their system and the cylindrical micelles, we hope that the constant A is principally [14] a characteristic of the materials; so, this interval has been used to evaluate the expressions 9 and 10. At this

point we assume that the presence of the salt does not modify drastically these values of A.

The attractive force per unit length (expression 10) are presented in Fig.6 for the two limit values of A as a function of D.

#### (C) FORCE BALANCE

For dissociation constants ( $\alpha$ ) greater or equal to 0.1, there are equilibrium points between the forces, i.e., the total force vanishes. At the interval  $0.1 \leq \alpha \leq 1$  the equilibrium points are placed between 50 and 58Å. (for  $A = 3.4 \times 10^{-14}$  erg) and at the interval  $0.15 \leq \alpha \leq 1$  between 45 and 51Å (for  $A = 6.8 \times 10^{-14}$  erg). Fixed the Hamaker constant, for  $\alpha \rightarrow 0$ , the equilibrium distance tends to the cylinder diameter (corresponding to the excluded volume interaction). This result indicates that equilibrium distances greater than 60Å are not to be expected in this simplified picture of two interacting cylinders. Modifications in the location of the equilibrium points could be expected in a many body interacting problem.

For  $\alpha \leq 0.1$  there is no equilibrium point between the two forces; the attractive force is bigger than the repulsive one and the system flocculates, with segregation of the free water unbounded to the micelles. This flocculation condition obtained for the two micelle system can reasonably be extended to the hole system.

The value of 49.9Å for the lattice parameter [10] of the hexagonal array can be explained considering the solvation water [15] bound to the micelles. The micelles

surface is composed basically by hydrophilic groups and it is involved by anionic cloud of counter ions, all of them solvated by water molecules. A solvation shell approximately  $8\text{\AA}$  thick (i.e. of the order of 3 aligned water molecules) per micelle gives an effective radius of about  $25\text{\AA}$  and a lattice parameter of  $50\text{\AA}$ . This water molecules are directly bounded to the micelles hydrophilic groups or to the counter ions that makes the electrostatic screening so, this solvation shell can be thought as a constitutive part of the micelles, that have then a greater effective radius.

It is interesting to study the process of formation of the aggregates in terms of the total energy of the two cylinders, by summation of the expressions 7 and 9. These results are plotted in Fig.7 for different values of  $\alpha$  (and  $A = 3.4 \times 10^{-14}$  erg) in units of  $KT$  ( $T = 298^\circ\text{K}$ ) per centimeter. For  $\alpha > 0.1$  there are equilibrium points at the potential well, however with energy smaller than  $KT$ . For  $\alpha < 0.1$  the attractive interaction dominates. In Fig.8 it is plotted the total energy for  $\alpha = 0.02$  and the two limit values for the Hamaker constant. Assuming for the micelle length the value of  $10^3\text{\AA}$  [10,29], at  $50\text{\AA}$  of interaxial distance the total energy of the system is located between  $0.64\text{ KT}$  and  $1.35\text{ KT}$ ; for  $\alpha = 0$  the total energy coincides with the attractive energy and is located between  $0.68\text{ KT}$  and  $1.37\text{ KT}$ . This energy, very close to  $KT$ , could justify the necessity of external agents [10], like fields and surface, to favour the nucleation of the micelles in large aggregates.

The wall effects, described qualitatively before, can be thought as a micellar anchoring process. The micelles, near the surface have their axes oriented

about the capillary axis and the anchoring process restricts some of their degrees of freedom and flocculation is favoured. The same process occurs in the parallel wall containers, differing only in terms of the preferred orientation present. The smaller the capillary diameter is, the larger the OB intensity compared to IB, until the formation of the aggregates of  $N \geq 400$ . The modification of the lattice parameter observed with samples in capillaries C1 and C2 could be explained by a small change of the solvation water shell involving the micelles, by influence of the container wall.

The results with surface treated capillaries also corroborate the picture where the segregation of the free water from the wall proximity favours the formation of the large aggregates. The lattice parameter observed remains, within the experimental error, the same as in untreated capillaries in spite of the increase in  $N$ .

Also the presence of a magnetic field, which makes the micelles stay parallel to each other, promotes a particular micellar geometry that favours the flocculation process.

## VI - CONCLUSIONS

The application of DLVO theory to "nematic" type I lyomesophase indicates that the system tends to flocculate due to the superiority of van der Waals attractive force compared to the coulombian repulsive interaction.

The lattice parameter of the hexagonal network obtained by X-ray diffraction results can be explained

assuming that the micelles have a solvation shell around them about  $8\text{\AA}$  thick (effective micellar radius about  $25\text{\AA}$ ). The balance between van der Waals attractive force and excluded volume interaction are responsible for the aggregation process. This process is counter balanced by thermal agitation; the energy of two flocculated micelles  $50\text{\AA}$  apart is about  $KT$  ( $T = 298^\circ\text{K}$ ). Apparently at the bulk of the mesophase there is a process where only small aggregates can exist; the large ones are formed by external agents like fields and wall containers. These agents act to restrict degrees of freedom of the micelles favouring the nucleation process. The container wall effect is a phenomenon of micellar anchoring and the surface induced hydrophobicity acts to exclude the free water from its proximity favouring the nucleation.

#### VII - ACKNOWLEDGEMENTS

We thank Dra. V.R.Paoli and Dr.J.A.Vanin for the preparations of the lyomesophase and many helpful discussions. The computational help of Mr.C.A.Carvalho is also acknowledged. FINEP, FAPESP and CNPq gave us imprescindible financial support.

#### REFERENCES

1. Radley, K., Reeves, L.W., and Tracey, A.S., 1976, J.Phys. Chem., 80, 174.
2. Fujiwara, F., Reeves, L.W., Suzuki, M., and Vanin, J.A., 1979, Solution Chemistry of Surfactants, ed. K. Mittal, vol.1, pp. 63-77 (Plenum Press, N.Y.)
3. Charvolin, J., Levelut, A.M., and Samulski, E.T., 1979, J. Physique Lett., 40, L587.
4. Radley, K. and Saupé, A., 1978, Mol. Cryst. Liq. Cryst. 44, 227; Mol. Phys., 35, 1405.
5. Charvolin, J. and Hendrikx, Y., 1980, J.Physique Lett., 41, L597.
6. Amaral, L.Q., Pimentel, C.A., and Tavares, M.R., 1978, Acta Cryst. A34(S4) S188.
7. Amaral, L.Q., Pimentel, C.A., Tavares, M.R., and Vanin, J.A., 1979, J.Phys. Chem., 71, 2940.
8. Amaral, L.Q., and Tavares, M.R., 1980, Mol. Cryst. Liq. Cryst. Lett., 56, 203.
9. Figueiredo Neto, A.M., and Amaral, L.Q., 1981, Mol.Cryst. Liq. Cryst., 74, 109.
10. Figueiredo Neto, A.M., and Amaral, L.Q., 1982, Preprint IFUSP/P-314.
11. Figueiredo Neto, A.M., 1981, Ph. D. Thesis, Universidade de São Paulo (UNPUBLISHED).
12. Figueiredo Neto, A.M., and Amaral, L.Q., 1982, Preprint IFUSP/P-320.

13. Verwey, E.J.W., and Overbeek, J.Th. G., 1948, Theory of Stability of Lyophobic Colloids (Elsevier).
14. Brenner, S.L., and Mc Quarrie, D.A., 1973, Biophys. J. 13, 301.
15. Ekwall, P., 1975, Advances in Liquid Crystals, ed. G.H. Brown, vol. 1, pp. 1-142 (Ac. Press. London).
16. Mc Quarrie, D.A., 1976, Statistical Mechanics, pp. 327-356, (Harper and Row).
17. Olivares, W., and Mc Quarrie, D.A., 1975, Biophys. J. 15, 143.
18. Kirkwood, J.G., and Poirier, J.C., 1954, J.Phys.Chem., 58, 591.
19. Fuoss, R.M., Katchalsky, A., and Lifson, S., 1951, Proc. Nat. Acad. Sci., 37, 579.
20. Hill, T.L., 1955, Archs. Biochem. Biophys., 57, 229.
21. Sparnaay, M.J., 1959, Rec. Trav. Chim.Pays-Bas Belg., 78, 680.
22. Horn, R.G., and Israelachvili, J.N., 1980, Chem. Phys. Lett., 71, 192.
23. Grimson, M.J., and Rickayzen, G., 1981, Mol.Phys., 44, 817.
24. Brenner, S.L., and Mc Quarrie, D.A., 1973, J.Theor.Biol., 39, 343.
25. Brenner, S.L., and Mc Quarrie, D.A., 1973, J.Colloid Interface Sci, 44, 298.
26. Waddington, T.C., 1959, Advances in Inorganic Chemistry and Radio-Chemistry, ed. H.J. Emeléus and A.J.Sharpe, vol. 1, pp. 157-221, (Ac.Press, N.Y.).
27. Ninham, B.W., and Parsegian, V.A., 1970, Biophys. J., 10, 646.
28. Gingell, D., and Parsegian, V.A., 1972, J.Theor.Biol., 36, 41.
29. Forrest, B.J., and Reeves, L.W., 1981, J.Am. Chem. Soc., 103, 1641.

FIGURE CAPTIONS

Figure 1: Small angle X-ray result with sample LK in 0.3 mm thick quartz capillary. The capillary is in vertical direction in the plane of the figure.

Figure 2: Small angle X-ray result with sample LK in 0.5 mm thick quartz capillary. The capillary is in vertical direction in the plane of the figure.

Figure 3: Small angle X-ray result with sample LK in a cylindrical container with very thin parallel walls of Niquel, with radius of 3 mm and 0.7 mm sample thickness. The axis of the cylinder is parallel to the beam and normal to the plane of the figure.

Figure 4: Small angle X-ray result with sample LK in 0.7 mm thick quartz capillary, treated with  $(H_3C)_2SiCl_2$ . The capillary is in vertical direction in the plane of the figure.

Figure 5: Small angle X-ray result with sample LK in 2 mm thick pyrex capillary, treated with  $(H_3C)_2SiCl_2$ . The capillary is in vertical direction in the plane of the figure.

Figure 6: Natural logarithm of the absolute value of the attractive force in CGS units (dashed curves) for two values of the Hamaker constant (A) and repulsive force in CGS units (solid curves) for different dissociation constants ( $0.02 \leq \alpha \leq 1$ ), as a function of the interaxial distance (D).

Figure 7: Total potential energy of two parallel cylindrical micelles immersed in an ionic bathing medium as a function of the interaxial distance (D) for different dissociation constants ( $0.02 \leq \alpha \leq 1$ ). Hamaker constant used  $A = 3.4 \times 10^{-14}$  erg.

Figure 8: Total potential energy of two parallel cylindrical micelles immersed in an ionic bathing medium as a function of the interaxial distance (D), for the two limit values of the Hamaker constant. Dissociation constant  $\alpha = 0.02$ .



FIG. 1

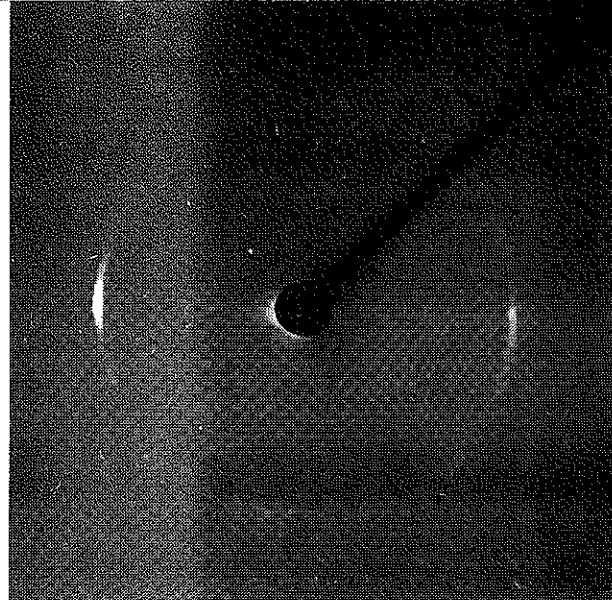


FIG. 2

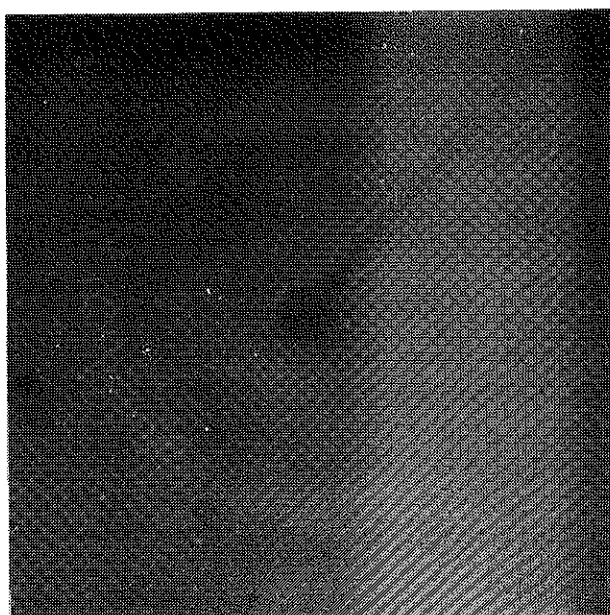


FIG. 3



FIG. 4



FIG. 5

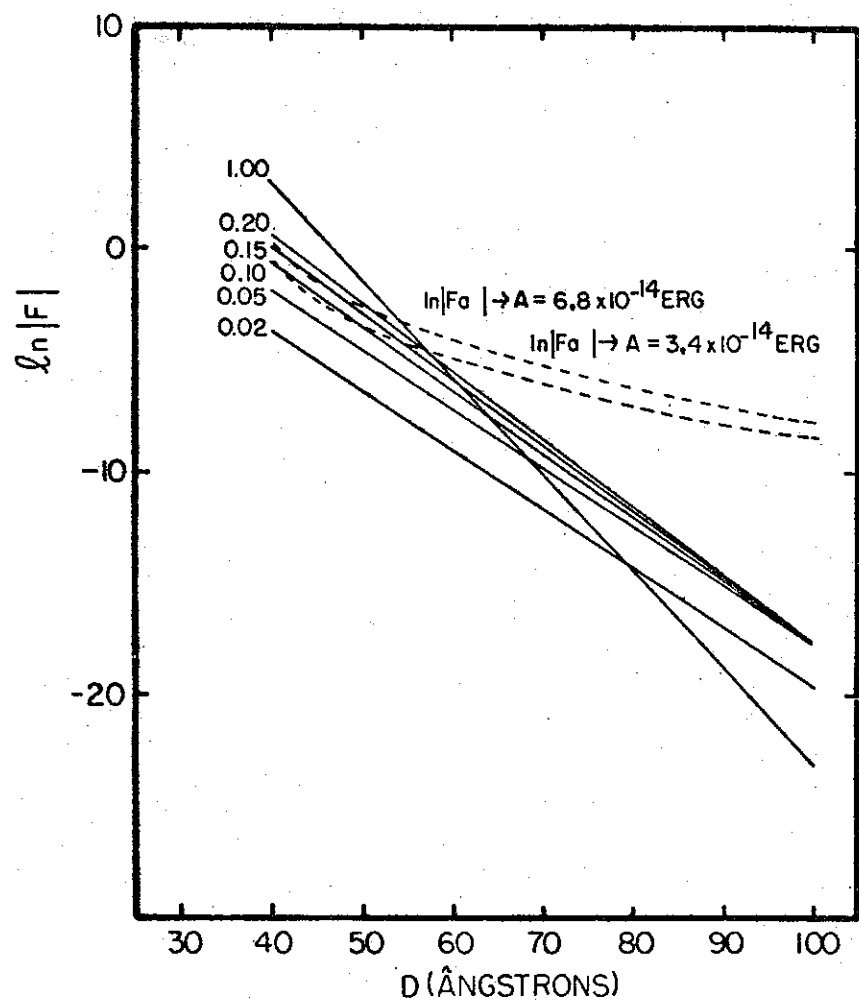
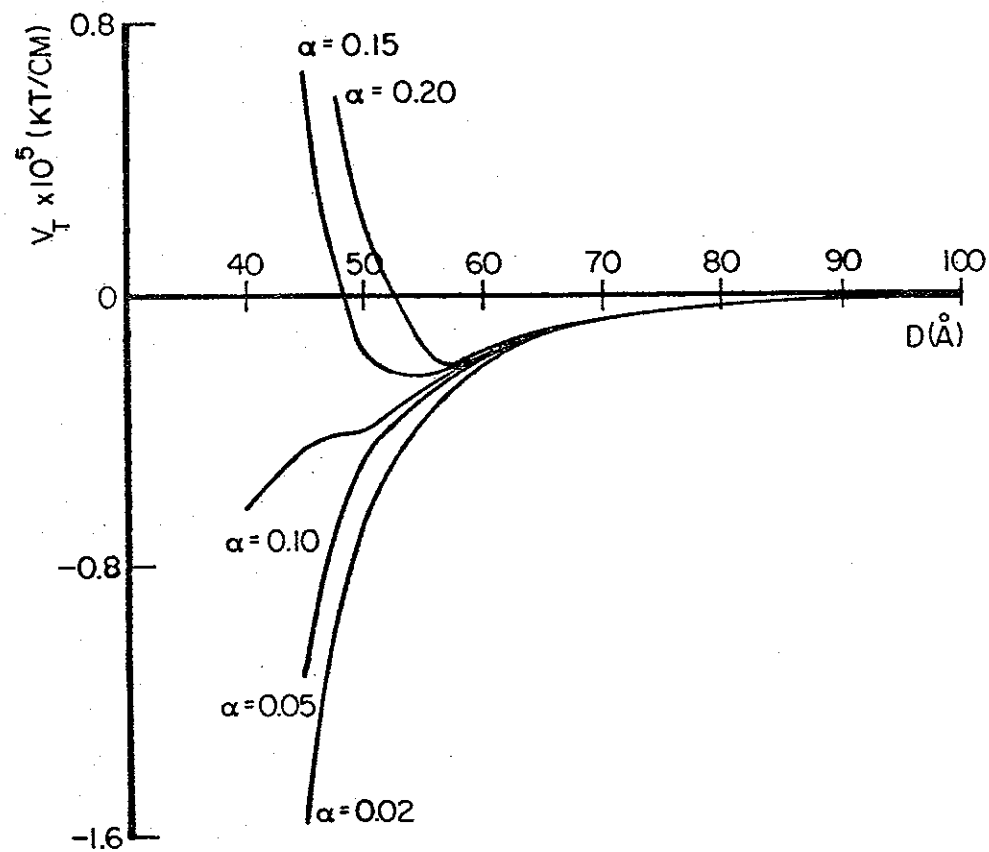


FIG. 6





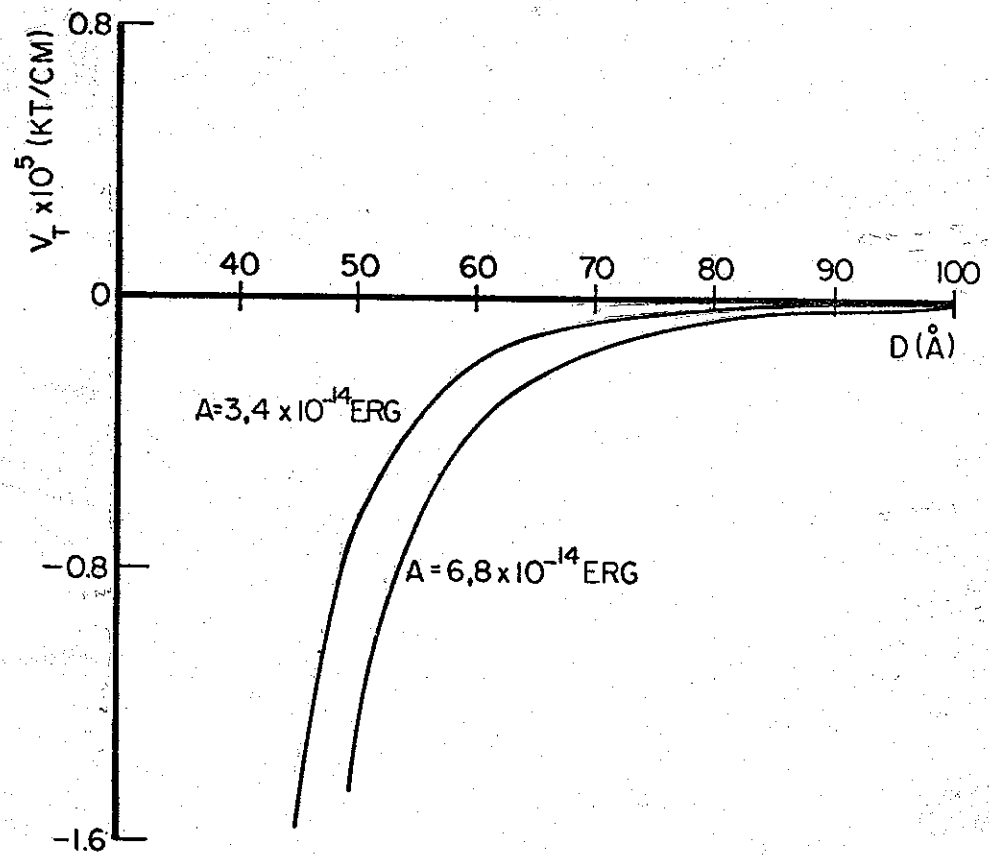


FIG. 8